J Therm Anal Calorim (2010) 102:451–460
DOI 10.1007/s10973-010-0935-1

PMMA/organomodified montmorillonite nanocomposites prepared by in situ bulk polymerization

Study of the reaction kinetics

Dimitris S. Achilias · Alexandros K. Nikolaidis · George P. Karayannidis

NATAS2009 Special Issue

Abstract Kinetics of the in situ bulk polymerization of methyl methacrylate in the presence of organomodified montmorillonite (MMT) was investigated using differential scanning calorimetry (DSC) and gravimetrically. Different amount and types of MMT under the trade names Cloisite were employed. Using DSC, the amount of heat released versus time, under isothermal conditions, was recorded, and eventually, the time evolution of polymerization rate and monomer conversion was calculated. Results on the variation of monomer conversion with reaction time were in good agreement to corresponding from the gravimetric measurements. The nanocomposites prepared were characterized with WAXD, TEM and FTIR, and their glass transition temperature, T_g, was measured with DSC. Depending on the added amount of nano-MMT, either exfoliated or intercalated structures were obtained. An enhancement of the polymerization rate with the presence of the nanoparticles was observed especially in the gel effect region. This was accompanied by a higher T_g and average molecular weight, as measured by GPC, of all nanocomposites compared to neat PMMA.

Keywords PMMA · Nanocomposites · Kinetics · DSC · In situ polymerization

D. S. Achilias (✉) · A. K. Nikolaidis · G. P. Karayannidis
Laboratory of Organic Chemical Technology, Department of Chemistry, Aristotle University of Thessaloniki, 541 24 Thessaloniki, Greece
e-mail: axilias@chem.auth.gr

Introduction

During the last 15 years, the study of polymer–inorganic nanocomposites has attracted the increasing interest of worldwide researchers, since they frequently exhibit unique hybrid physical and chemical properties, synergistically derived from the two components. Polymers reinforced with a small amount of montmorillonite (MMT) clay exhibit improved mechanical properties, high thermal stability, flame retardancy, as well as gas permeability resistance [1, 2]. The concept of polymer–clay nanocomposites was first introduced by researchers from Toyota [3], who discovered the possibility to build a nanocomposite from nylon-6 and organophilic clay. Their new material showed dramatic improvements in mechanical and physical properties. Numerous other researchers later used this concept for nanocomposites based on epoxies, unsaturated polyester, poly (1-caprolactone), poly (ethylene oxide), polystyrene, polyimide, polypropylene, poly (ethylene terephthalate) and polyurethane [1, 2]. Excellent reviews on polymer-layered silicate nanocomposites have been recently published [4–6]. From the structural point of view, two idealized polymer–clay nanocomposites are possible: intercalated and exfoliated [4]. Intercalation results from the penetration of polymer chains into the clay's interlayer region and interlayer expansion. Usually, the ordered layer structure is preserved and can be detected by X-ray diffraction (XRD). In contrast, exfoliation involves extensive polymer penetration and silicate crystallites delamination, and the individual nanometre-thick silicate platelets are randomly dispersed in the polymer matrix. Exfoliated nanocomposites usually provide the best property enhancement, due to the large aspect ratio and surface area of the clay. Moreover, since clay is naturally hydrophilic and inherently incompatible with most organic polymers, several

methods have been studied to make clay compatible with polymers. The most popular involves surface ion exchange, in which the metal cations on the clay's surface are exchanged for organic cationic surfactants typically ammonium or phosphonium compounds with long alkyl chains.

Poly(methyl methacrylate) (PMMA)/clay nanocomposites are of interest for improved thermal and mechanical properties, reduced flammability, reduced gas permeability, as well as their good potential to retain excellent optical clarity. Different preparation methods for PMMA/clay nanocomposites have been studied, including solution [7], or melt intercalation/exfoliation, [8–13] and in situ polymerization [14–18]. The last two methods being the most common ways of preparing the polymer–clay nanocomposites. While it is notoriously difficult to achieve a homogeneous distribution of nanometre-scale particles in highly viscous polymer melts, and aggregation of the particles cannot be avoided, dispersion in a suitable monomer followed by in situ polymerization is an attractive alternative route. In this technique, the modified layered silicate is swollen by a liquid monomer or a monomer solution. The monomer migrates into the galleries of the layered silicate, so that the polymerization reaction can occur between the intercalated sheets. Under conditions in which intra- and extragallery polymerization rates are properly balanced, the clay layers are delaminated and highly exfoliated nanocomposites are formed [5].

The literature on the in situ polymerization technique and reaction kinetics is briefly discussed next. In 2003, Li et al. [14] synthesized PMMA/MMT nanocomposites via in situ intercalative polymerization. The nanocomposites possessed partially exfoliated and partially intercalated structure, while their thermal stability, glass transition temperature (T_g) and mechanical properties were notably improved in comparison with pure PMMA. Moreover, the T_g and the thermal decomposition temperature of the nanocomposites prepared by Xie et al. [15] were 6–15 °C and 100–120 °C higher than those of pure PMMA. Su et al., [16] studied the effect of the clay organic modifier on the nanocomposites properties. Either exfoliated or intercalated systems were obtained with improved thermal stability. Ingram et al. [17] concluded that polymerization was accelerated in the presence of organoclay and that T_g was increased by 20 °C with only a few weight percent of clay. Qu et al. [18] also reported a substantial enhancement of the thermal stability and the mechanical properties of the nanocomposites that they produced. Finally, Dhibar et al. [19] investigated the effect of the manufacturing technique on the thermal and mechanical properties of PMMA–clay nanocomposites. Maximum T_g increment and better thermal stability were achieved by the in situ polymerization method.

While it is tacitly assumed that inorganic particles are not interfering with the mechanism of free-radical polymerization, it has been shown that this is not true. For example, in the bulk polymerization of methyl methacrylate (MMA) in the presence of nanometre-scaled ZnO, it was found that hydroxy groups on the ZnO surface may induce a degenerative transfer suppressing the gel effect during polymerization [20]. The average molecular weight of PMMA/SiO_2 nanocomposites was found either to increase or decrease compared to neat PMMA depending on the silica modification [21]. Xie et al. [22] concluded that nano-sized Sb_2O_3 particles do not inhibit polymerization of MMA during in situ MMA/Sb_2O_3 polymerization. The effect of different reaction parameters on the conversion of MMA in the presence of nano-$CaCO_3$ was studied by Wu et al. [23]. They found that the rate of polymerization increases apparently in the presence of nano-$CaCO_3$ particles. Concerning other polymers, use of an organomodified MMT was found to advance the curing kinetics of epoxy resins [24] and to result in slightly higher maximum degrees of conversion for UV-cured dimethacrylate-based nanocomposites [25]. Also, use of silica nanoparticles at concentrations less than 1 wt%, during the solid state polycondensation of poly(ethylene terephthalate) was found to result in higher intrinsic viscosity values, compared to neat PET at all reaction times [26]. Finally, size of nanoparticles has been found to play an important role especially when silica is used. In PMMA/silica nanocomposites, the degree of degradation improvement was found to increase linearly with the surface area of SiO_2 [27].

Based on the above literature survey, an effort was undertaken in this study to investigate if free-radical polymerization kinetics of MMA is affected by the presence of MMT nanoparticles. Reaction kinetics was measured using differential scanning calorimetry (DSC) by recording the amount of heat released versus time under isothermal conditions and eventually calculating the time evolution of polymerization rate and monomer conversion. Thermal analysis has been proved a useful tool for investigating the properties of polymer–clay nanocomposites [28] and macromolecular structure [29]. DSC has the advantages of employing very small amounts of reactants and constant reaction conditions (i.e., temperature) [30]. Another widely used technique to monitor monomer conversion during polymerization is to directly measure the polymer weight formed at pre-specified time intervals and divided it over the initial monomer weight. This method, although absolute, has the disadvantage of non-achieving adequate isothermal conditions during the reaction, especially in monomers with strong effect of diffusion-controlled phenomena. However, there still remains the advantage of having polymer samples at different time

intervals. In this article, both methods were used, and comparative results were presented. The nanocomposites produced were characterized with wide-angle X-ray diffraction (WAXD), transmission electron microscopy (TEM) and Fourier-transform infra-red analysis (FTIR), their molecular weight distribution was measured with gel permeation chromatography (GPC) and their glass transition temperature with the DSC.

Experimental

Materials

The methyl methacrylate monomer used was purchased from Fluka and the hydroquinone inhibitor was removed by passing it, at least twice, through a disposable inhibitor-remover packed column (from Aldrich). The polymerization initiator benzoyl peroxide (BPO) was provided by Fluka and purified by fractional recrystallization twice from methanol (purchased from Merck). CH_2Cl_2 was used as a polymer solvent from Merck, while methanol used for the polymer re-precipitation was also supplied from Merck. All other chemicals used were of reagent grade.

For the preparation of the nanocomposites, commercial organically modified montmorillonite (OMMT) clays, Cloisite 15A, Cloisite 25A and Cloisite 30B were used and kindly provided by Southern Clay Products Inc. (Texas, USA). These are MMT modified with a quaternary ammonium salt, which is dimethyl hydrogenated tallow (cationic exchange capacity of 125 meq per 100 g clay), dimethyl 2-ethyl hexyl hydrogenated tallow (CEC 95 meq per 100 g clay) and methyl tallow bis-2-hydroxyethyl (CEC 90 meq per 100 g clay) for Cloisite 15A, 25A and 30B, respectively. The chemical structure of the ammonium salts follows:

Cloisite 15A

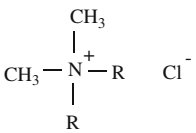

Cloisite 25A

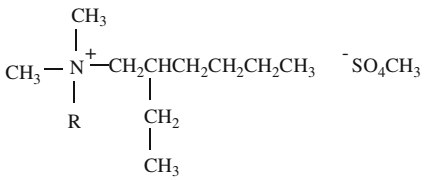

Cloisite 30B

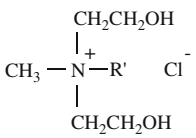

R and R′ are hydrogenated tallow and tallow (~65% C18, ~30% C16, ~5% C14), respectively.

Typical physical properties according to the manufacturer were the following: size as measured by a transmission electron microscope for a PA6 nanocomposite 75–150 nm × 1 nm and surface area 750 $m^2\ g^{-1}$ when exfoliated. In addition, sodium containing natural MMT was used under the trade name Cloisite Na^+ and CEC = 92 meq per 100 g MMT [31].

Preparation of the initial monomer–nanoclay mixtures

The initial mixture was prepared by dispersing the appropriate amount of OMMT (usually 0.25 g) in 25 g of the monomer MMA in a 100-mL conical flask (composition 1 wt% MMT) by adequate magnetic and supersonic agitation. The duration of agitation was varied with the type of MMT used. Thus, the magnetic agitation for the Cloisite Na^+, Cloisite 15A, Cloisite 25A and Cloisite 30B lasted for 24, 2, 15 and 22.5 h, respectively, while the supersonic agitation was 1 h for all samples. The dispersion of the nanoparticles in the monomer was homogeneous, as indicated by the high translucency in the visible region. In the final suspension, the initiator benzoyl peroxide (BPO) was added (0.1926 g corresponding to 0.03 M) under magnetic agitation for 5 min, and the mixture was degassed by passing nitrogen and immediately used.

Polymerization

The bulk free-radical polymerization of MMA was investigated using the DSC-Diamond (Perkin-Elmer). Approximately 10–15 mg of each sample were weighed, put into the standard Perkin-Elmer sample pan, sealed and placed into the appropriate position of the instrument. Polymerizations were conducted at 80 °C. The reaction temperature was monitored and maintained constant (within ±0.01 °C) during the whole conversion range. The reaction exotherm (in normalized values, W g^{-1}) at a constant temperature was recorded as a function of time. The rate of heat release ($d(\Delta H)/dt$) measured by the DSC was directly converted into the overall reaction rate (dx/dt) using the following formula:

$$\frac{dx}{dt} = \frac{1}{\Delta H_T}\frac{d(\Delta H)}{dt}, \quad (1)$$

where ΔH_T denotes the total heat released if all double bonds reacted.

Polymerization enthalpy and conversion were calculated by integrating the area between the DSC thermograms and the baseline established by extrapolation from the trace produced after complete polymerization (no change in the heat produced during the reaction). The residual monomer content and the total reaction enthalpy, ΔH_T, were determined by heating the sample from the polymerization temperature to 180 °C at a rate of 10 K min^{-1}. The sum of enthalpies of the isothermal, ΔH_R, plus the dynamic experiment, ΔH_D, was the total reaction enthalpy. By dividing ΔH_R over ΔH_T the ultimate degree of conversion, X_{max}, could be estimated.

Following, the samples were cooled to 20 °C and their glass transition temperature was measured by heating to 180 °C at a rate of 10 K min^{-1}.

In addition to the polymerizations carried out in the DSC, similar experiments with exactly the same initial monomer–nanoclay–initiator composition were carried out in small test-tubes to have nanocomposites at different reaction time intervals. According to this technique, 2 mL of the pre-weighted mixtures of monomer with the initiator and each Cloisite were placed into a series of 10 test-tubes. After degassing with nitrogen they were sealed and placed into a pre-heated bath at 80 °C. Each test-tube was removed from the bath at 6 min time intervals and was immediately frozen to stop the reaction. The product was isolated after dissolution in CH_2Cl_2 and re-precipitation in MeOH. The polymers were dried to constant weight in a vacuum oven at room temperature. All final samples were weighed, and the degree of conversion was estimated gravimetrically.

Measurements

Fourier-transform infra-red (FTIR)

The chemical structure of the PMMA-based nanocomposites and different Cloisites, was confirmed by recording their IR spectra. The instrument used was an FTIR spectrophotometer of Perkin-Elmer, Spectrum One. The resolution of the equipment was 4 cm^{-1}. The recorded wavenumber range was from 400 to 4000 cm^{-1} and 32 spectra were averaged to reduce the noise. A commercial software Spectrum v5.0.1 (Perkin-Elmer LLC 1500F2429) was used to process and calculate all the data from the spectra. Thin polymeric nanocomposite films were used in each measurement, formed by a hydraulic press Paul-Otto Weber, at a temperature 170 °C.

Wide angle X-ray diffraction (WAXD)

X-ray diffraction patterns were obtained using an X-ray diffractometer (3003 TT, Rich. Seifert) equipped with Cu K_α generator ($\lambda = 0.1540$ nm). Scans were taken in the range of the diffraction angle $2\theta = 1°$–$10°$.

Transmission electron microscopy (TEM)

Transmission electron microscopy (TEM) experiments were carried out on a JEOL 2011 TEM with a LaB6 filament and an accelerating voltage of 200 kV. Samples were prepared by evaporating drops of a PMMA/OMMT nanocomposite–ethanol suspension after sonication onto a carbon-coated lacy film supported on a 3 mm diameter, 300 mesh copper grid.

Gel permeation chromatography (GPC)

The molecular weight distribution and the average molecular weights of pristine PMMA and all nanocomposites were determined by GPC. The instrument used was from Polymer Laboratories, model PL-GPC 50 Plus and included an isocratic pump, a differential refractive index detector and three PLgel 5μ MIXED-C columns in series. All samples were dissolved in THF at a constant concentration of 1 mg mL^{-1}. After filtration, 200 μL of each sample was injected into the chromatograph. The elution solvent was THF at a constant flow rate of 1 mL min^{-1}, and all the systems were at constant temperature 30 °C. Calibration of GPC was carried out with standard poly(methyl methacrylate) samples (Polymer Laboratories) with peak molecular weight ranging from 690 to 1944000.

Results and discussion

Polymer–clay nanocomposites could be characterized as immiscible, intercalated, partially exfoliated or exfoliated. The particular form depends on the clay content, the chemical nature of the organic modifier, and the synthetic method. In general, an exfoliated system is more feasible with lower clay content (about 1 wt%), while an intercalated structure is frequently observed for nanocomposites with higher clay content. XRD results for pure PMMA and all PMMA nanocomposites with different Cloisites appear in Fig. 1. No significant peak was found for pure PMMA and PMMA nanocomposites, except for a small peak around 2.4° (corresponding to $d = 3.5$ nm) observed in the nanocomposite containing Cloisite 15A. Thus, from the XRD patterns, it is suggested that all nanocomposites obtained from the in situ bulk polymerization are exfoliated except from this with the Cloisite 15A, which could be considered as partially exfoliated and intercalated. Similar behaviour has been reported in literature for nanocomposites of PMMA with Cloisite 93A [32], Cloisite 30B [17] and Cloisite Na^+ [18].

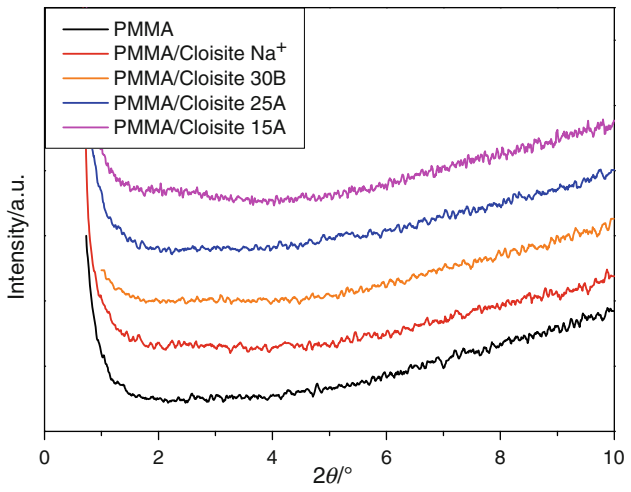

Fig. 1 Comparative XRD spectra of PMMA and PMMA nanocomposites with Cloisite Na^+, Cloisite 15A, Cloisite 25A and Cloisite 30B obtained from the bulk polymerization of MMA with different OMMT nanoparticles at a weight fraction of 1 wt%, constant temperature of 80 °C and initial initiator concentration 0.03 M BPO

TEM observations were used to augment WAXD analysis of the nanostructures. Figure 2 shows an indicative TEM micrograph of the PMMA/Cloisite 30B nanocomposite, where the brighter region represents the polymer matrix while the dark narrow stripes represent the MMT nanoparticles. Notice that in order to distinguish between intercalated or exfoliated structures, a high magnification has been employed. This figure reveals that individual layers of the MMT are well dispersed in the PMMA matrix and separated one from the other. This means that OMMT was exfoliated into secondary particles with a thickness lower than 20 nm.

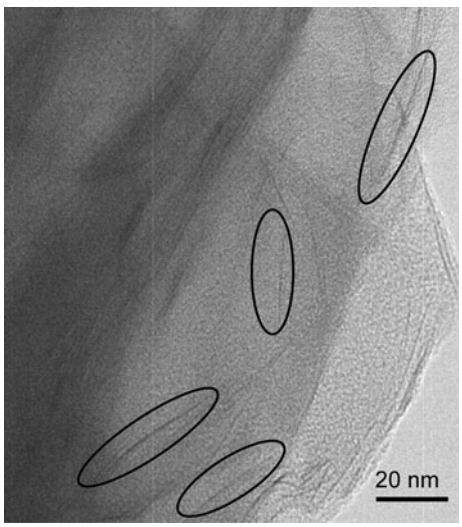

Fig. 2 TEM micrograph of PMMA–Cloisite 30B nanocomposite exhibiting exfoliated OMMT

Another measurement carried out to denote the uniform distribution of the nano-clay in the polymer matrix was that of FTIR spectroscopy. Therefore, the FT-IR spectra of all nanocomposites were recorded and compared to pure PMMA and the corresponding nano-clay. Results are presented in Fig. 3a–d for all nanocomposites. Very distinctive is the characteristic absorption at 1735 cm^{-1} due to the stretching of the carbonyl bond (C=O). It was observed that the spectra of all nanocomposites have the same peaks with those of pure PMMA, as well as some additional small peaks coming from the OMMT (i.e., the bonds of Si–O and Mg–O). Therefore, the appearance of the nano-clay in the polymer matrix was confirmed.

Results on conversion versus time for pure PMMA and the nanocomposites, obtained from the test-tube experiments, appear in Fig. 4. As it can be seen, the reaction does not reach complete conversion but an ultimate conversion around 96–97%. This is due to the well-known glass effect, which is due to the effect of diffusion-controlled phenomena on the propagation reaction and the reduced mobility of monomer molecules to find a macro-radical and react [33–35]. In this stage, reaction rate is almost zero although there are some unreacted monomer molecules. Besides, in all cases, the auto-acceleration phenomenon was also observed (denoted from an abrupt increase in the conversion values), starting at 20–30% conversion. This is attributed to the effect of diffusion-controlled phenomena on the termination reaction and the reduced mobility of live macro-radicals to find one another and react. Therefore, their concentration increases, leading in increased reaction rates. However, from these initial results, it seems that this phenomenon starts earlier in the nanocomposites with the OMMT and does not seem to depend on the type of modification. Similar results have been also reported in literature [17]. From the results of Fig. 4b, it was observed that the composition of 1 wt% OMMT seems to result in a higher conversion rate and this was followed in all subsequent experiments. Another interesting observation was that at high amounts of OMMT (i.e., 5%), the final conversion was less than the others meaning that increased amount of clay leads to a more pronounced decrease in the movement of the small monomer molecules so that their diffusion becomes restricted and they do not easily react. A diagram illustrating these results has been presented in a previous publication [36].

Further experimental conversion versus time results were obtained using the DSC technique. In order to test the reliability of both experimental measurements, results on monomer conversion as a function of time obtained from two methods were compared. Exactly the same experiment, using the same experimental conditions and materials, was repeated twice, in the DSC and the test-tubes. Polymerization rate data taken from the DSC were converted to

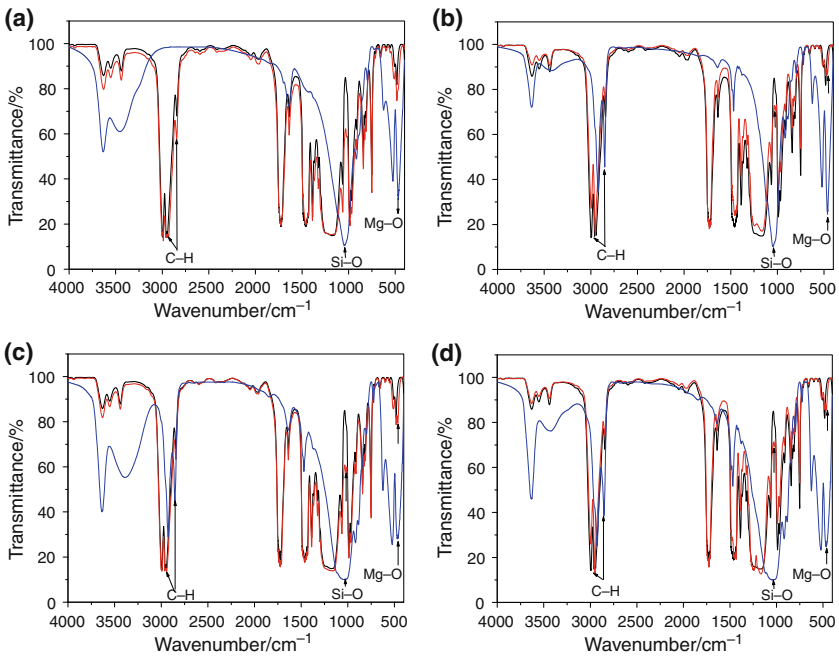

Fig. 3 Comparative FT-IR spectra of neat PMMA (*black line*), PMMA nanocomposites with Cloisite Na^+ (**a**), Cloisite 15A (**b**), Cloisite 30B (**c**) and Cloisite 25A (**d**) (*red line*) and neat nano-filler (*blue line*), respectively obtained from the in situ bulk polymerization of MMA with different OMMT nanoparticles at a weight fraction of 1 wt%, constant temperature 80 °C and initial initiator concentration 0.03 M BPO. (Color figure online)

conversion versus time and appear in Fig. 5, together with the gravimetric measurements for the PMMA–Cloisite Na^+ nanocomposite. As it can be seen, despite the fact that DSC provides double bond conversion, while gravimetric measurements represent direct polymer weight, results are in very good agreement. An overestimation of conversion obtained from the test-tubes experiments was observed compared to the DSC results, in the conversion values between 20 and 80%, where the gel effect appears and reaction rate increases rapidly. This is attributed to a possible slight local increase in temperature inside the test-tubes caused by the strong reaction exotherm, which could not be balanced in the constant temperature bath where the test-tubes were placed. In contrast, the polymerization in the DSC pans could be considered as totally isothermal due to the small sample mass and the adequate heat control of the instrument [37].

Overall, application of the DSC in monitoring the free-radical polymerization reaction kinetics presents the following advantages compared to gravimetric experiments [30, 37]: use of very small amounts (a few mg) of reaction mixtures (monomer/initiator); achievement of isothermal conditions during polymerization even when strong auto-acceleration effect is present; ability of continuous monitoring the reaction and not taking only discrete experimental data at pre-specific time intervals; easy application in polymerizations leading in crosslinked networks where the application of other techniques is very difficult; intrinsic phenomena like gel effect are more easily distinguishable; very fast polymerization reactions completed in a few minutes can be easily followed; possibility of performing non-isothermal experiments, which could lead in process optimization. Limitations of the DSC technique include not adequate removal of the amount of oxygen in monomer or trapped in the reaction pan leading to the appearance of an induction time due to the inhibition effect. When using volatile solvents the reaction temperature is usually limited by its boiling point, since possible evaporation could lead in a mass loss and alteration of the results. Use of specially designed pans hermetically sealed could avoid this limitation. Finally, as a limitation it could be considered that since samples are not collected at discrete time intervals, the method is not adequate when the variation of properties changing during reaction (i.e., molecular weight distribution, or copolymer composition, etc.) is needed.

Results showing the effect of the type of MMT on the reaction rate and conversion versus time, measured from the DSC experiments, are presented in Fig. 6a and b, respectively. The shape of the reaction rate curve is almost the same for all nanocomposites and exhibits all the characteristics of free-radical polymerization with strong effect of diffusion-controlled phenomena on the reaction mechanism [33]. The main characteristics include a large increase in the reaction rate curve in the gel effect region, followed by a decrease to almost zero before complete polymerization, due to the gel and glass effect, respectively. However, it seems that the great reaction exotherm, due to the auto-acceleration phenomenon (gel effect), is taking place earlier in the case of the OMMT nanomaterials. The same is obvious in the conversion versus time curves, where it seems that the reaction stops earlier compared to the reference sample (MMA without particles). One possible explanation could be provided if

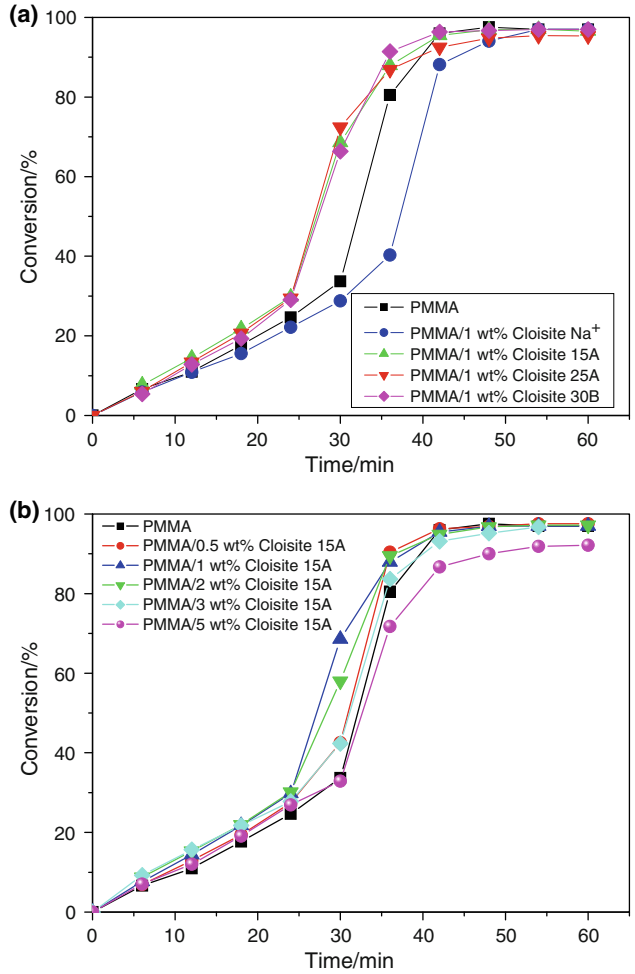

Fig. 4 Effect of the type (**a**) and the amount (**b**) of nano-MMT on the conversion versus time during bulk polymerization of MMA with 0.03 M BPO at 80 °C (test-tube experiments)

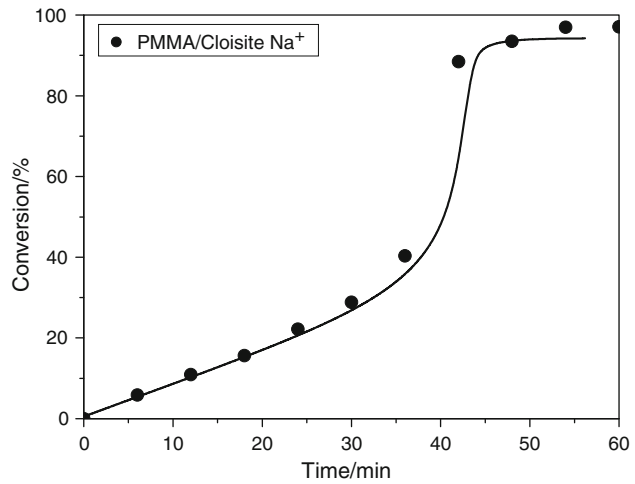

Fig. 5 Comparison of conversion versus time values obtained from test-tube experiments (*discrete points*) and the DSC (*continuous line*) for the PMMA–Cloisite Na^+ nanocomposite polymerized at 80 °C with initiator BPO 0.03 M

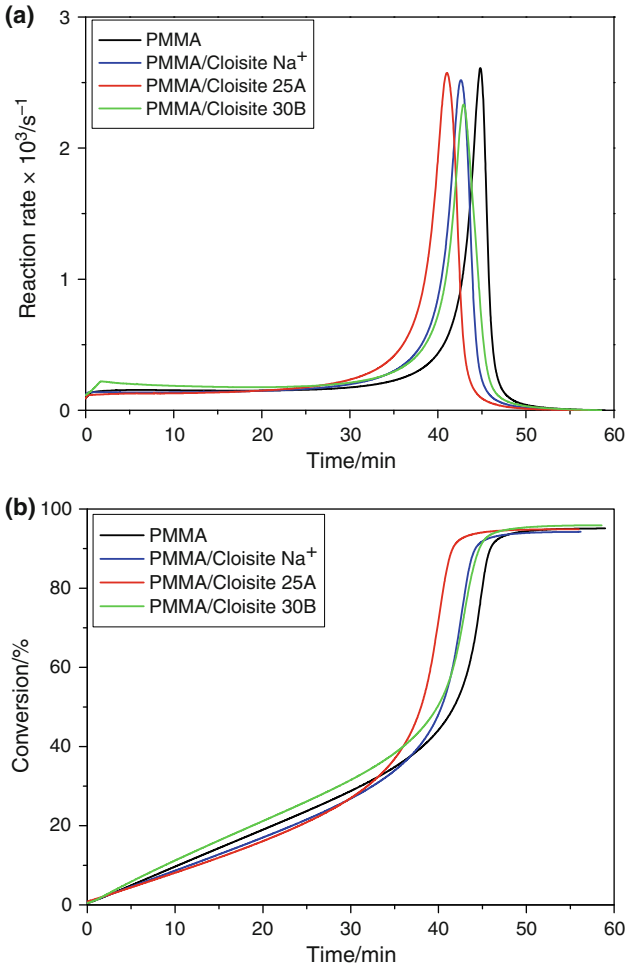

Fig. 6 Reaction rate (**a**) and conversion (**b**) versus time during bulk polymerization of MMA with different OMMT nanoparticles at a weight fraction of 1 wt%, constant temperature of 80 °C and initial initiator concentration 0.03 M BPO

we consider the organic modifiers (ammonium salts) used in each Cloisite. From the chemical structures provided in the experimental section, it seems that all organic modifiers constitute of large molecules. Therefore, it could be postulated that this large chemical structures hinder the movement of macro-radicals in space to find one another and react, resulting in increased radical concentrations. This is exactly the cause of the gel effect. Thus, it appears that the presence of OMMT nanoparticles enhances the rate of polymerization and slightly shortens the polymerization time to achieve a specific monomer conversion.

At this point, it was interesting to recall some principles from free-radical polymerization kinetics as it has been described in several textbooks [30, 38]. A simple mechanism of free-radical polymerization can be derived in terms of the following four elementary reactions:

$$\text{Initiation}: \quad I \xrightarrow{k_d} 2I^{\bullet}$$

$$I^{\bullet} + M \xrightarrow{k_I} R_1^{\bullet}$$

$$\text{Propagation}: \quad R_n^{\bullet} + M \xrightarrow{k_p} R_{n+1}^{\bullet}$$

$$\text{Chain transfer to monomer}: \quad R_n^{\bullet} + M \xrightarrow{k_{tr,m}} R_1^{\bullet} + D_n$$

Termination by combination/disproportionation :

$$R_n^{\bullet} + R_m^{\bullet} \begin{cases} \xrightarrow{k_{tc}} D_{n+m} \\ \xrightarrow{k_{td}} D_n + D_m \end{cases}$$

In the above kinetic scheme, the symbols I, $I^{\bullet}$ and M denote the initiator, radicals formed by the fragmentation of the initiator and monomer molecules, respectively. The symbols $R_n^{\bullet}$ and D_n are used to identify the respective "live" macroradicals and the "dead" polymer chains, containing n monomer structural units. Finally, k_d, k_p, $k_{tr,m}$, k_{tc} and k_{td}, denote the respective rate constants of the initiator decomposition, propagation, chain transfer to monomer, termination by combination and termination by disproportionation reactions.

According to the above kinetic scheme and assuming the quasi-steady-state-approximation for the free-radical concentration, the overall reaction rate, R_p, is given by

$$R_p = -\frac{d[M]}{dt} = k_p[M]\left(\frac{fk_d[I]}{k_t}\right)^{1/2} \Rightarrow \frac{dX}{dt} = k_p(1-X)\left(\frac{fk_d[I]}{k_t}\right)^{1/2}, \quad (2)$$

where X denotes fractional monomer conversion

Equation 2 can be integrated assuming that all kinetic rate constants and initiator efficiency are constant to yield an expression which directly correlates the monomer conversion with an observed overall kinetic rate coefficient, k. It should be noted that Eq. 3 is valid only for low degrees of monomer conversion:

$$-\ln(1-X) = kt; \quad k = k_p\left(\frac{fk_d}{k_t}\right)^{1/2}[I]^{1/2}. \quad (3)$$

The overall kinetic rate constant, k, can be obtained from the slope of the initial linear part of the plot of $-\ln(1-X)$ versus t. Such plots at conversion values in between 1 and 20% (i.e., $1\% < X < 20\%$) appear in Fig. 7. The lowest limit was taken such as to eliminate the inhibition period, while the highest value was well below the onset of diffusion-controlled phenomena. The experimental data fit very well to straight lines for all different nanocomposites, indicating the validity of Eq. 3 in the specific conversion interval. The values of k thus estimated are illustrated in Table 1. The results showed that the k value for neat PMMA was slightly higher than that with the Cloisite Na^+, while

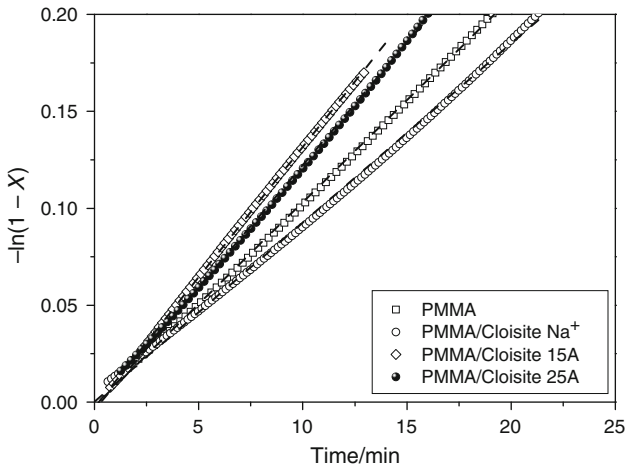

Fig. 7 Plot of $-\ln(1-X)$ versus time for the bulk polymerization of MMA with different OMMT nanoparticles at a weight fraction of 1 wt%, constant temperature of 80 °C and initial initiator concentration 0.03 M BPO

Table 1 Amount of heat released during reaction, ΔH_R, amount of heat released during the second dynamic step, ΔH_D, ultimate degree of conversion, X_{max}, overall kinetic rate constant, k, and glass transition temperature, T_g, for all nanocomposites investigated

Sample	ΔH_R/J g^{-1}	ΔH_D/J g^{-1}	X_{max}/%	k/min^{-1}	T_g/°C
PMMA	513.5	26.5	95.1	0.0105	100.6
PMMA/ Cloisite Na^+	455.3	27.9	94.2	0.0095	117.8
PMMA/ Cloisite 15A	456.4	19.6	95.9	0.0135	118.2
PMMA/ Cloisite 25A	450.9	24.1	94.9	0.0129	117.7
PMMA/ Cloisite 30B	504.1	21.3	95.9	0.0132	116.4

lower than all other nanocomposites with Cloisite 15A, 25A and 30B. The latter exhibits similar k values within experimental error.

Furthermore, the application of DSC in determining the onset of the effect of diffusion-controlled phenomena on polymerization rate is demonstrated. From a rearrangement of Eq. 2, the following Eq. 4 results

$$R_p = \frac{dX}{dt} = k_p\left(\frac{fk_d}{k_t}\right)^{1/2}[I]^{1/2}(1-X) = k'[I]^{1/2}(1-X) \cong k(1-X) \Rightarrow \frac{R_p}{(1-X)} = k. \quad (4)$$

In the absence of diffusion-controlled phenomena on the propagation and termination rate constants, as well as negligible initiator consumption, by plotting $R_p/(1-X)$ versus conversion or time, a straight line parallel to the x-axis should be obtained. A deviation from a constant

value is indicative of the existence of the effect of diffusion-controlled phenomena on the reaction kinetics. Such a plot appears in Fig. 8. As it can be seen, initially a constant value holds for k until 20–25% conversion. The point where this line deviates from the initial constant value denotes the onset of diffusion-controlled phenomena (gel effect). This value range is lower to the corresponding values estimated by other techniques (for example, by taking the deviation from linearity of the $-\ln(1 - X)$ vs. time curve). It was noted that the PMMA–Cloisite 25A nanocomposite exhibits an earlier start of the gel effect and higher values of reaction rate during its evolution.

With the DSC, it was also measured the amount of heat released during reaction, ΔH_R, as well as that released during the second non-isothermal stage, ΔH_D. These values for all nanocomposites are illustrated in Table 1. By dividing these values, the ultimate conversion, X_{max} can be obtained and these values are also tabulated in the same table. Within experimental error the existence of the nanoparticles does not seem to affect the ultimate degree of conversion.

Another "nano-effect" noted in the literature has been the change in the T_g of the polymer matrix with the addition of nanosized particles. Both increase and decrease in the T_g have been reported dependant upon the interaction between the matrix and the particle [4]. In most literature examples where T_g values have been obtained, usually only modest changes are reported (<10 °C). In some cases, the organic modification of clay can result in a decrease in T_g due to plasticization [13]. The method used for the nanocomposite formation (i.e., solution, melt or in situ polymerization) has been shown also to affect T_g, with the in situ polymerization giving the higher value (116 °C compared to 99 °C for neat PMMA) [19]. The T_g of the nanocomposites produced was measured with the DSC and

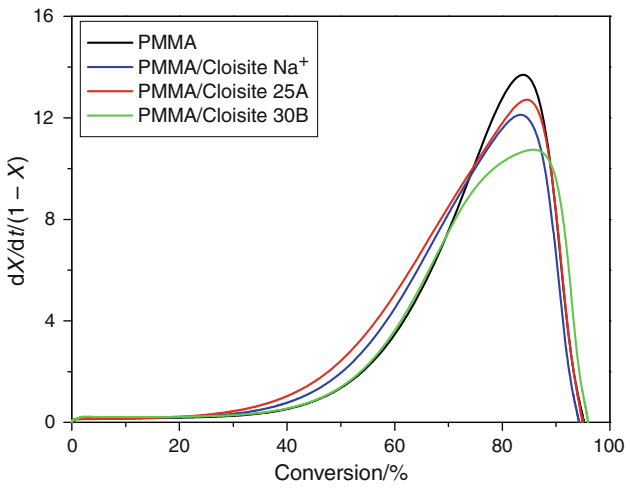

Fig. 8 Variation of $(dX/dt)/(1 - X)$ with conversion for all nanocomposites. Experimental details are as in Fig. 5

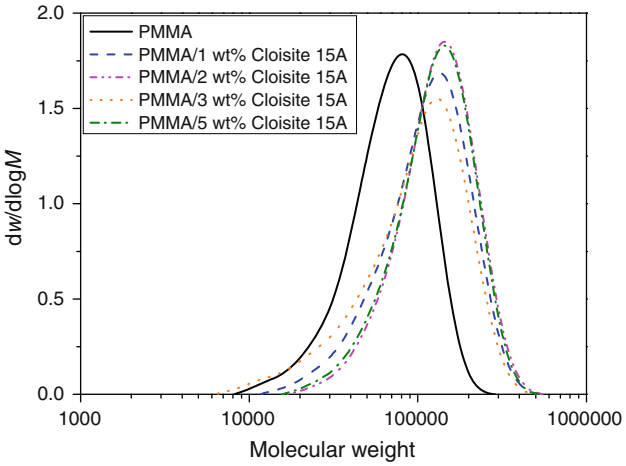

Fig. 9 Molecular weight distribution of neat PMMA and PMMA nanocomposites

found to be around 118 °C (Table 1) higher than the corresponding of neat PMMA (101 °C), in close agreement to literature values [7, 13, 14, 18]. This is ascribed to the confinement of intercalated PMMA chains within the silicate galleries that prevents the segmental motions of the polymer chains [7]. Another reason could be the higher average molecular weight that all nanocomposites exhibited compared to neat PMMA. As it can be seen in Fig. 9, the full MWD of all nanocomposites is shifted to higher values compared to neat PMMA. The number average molecular weight of neat PMMA, PMMA/Cloisite Na^+, PMMA/Cloisite 15A, PMMA-Cloisite 25A and PMMA-Cloisite 30B was 56930, 68720, 69830, 64850 and 63220, respectively. This in turn can be explained by the increase in the length of the macro-radicals before they find one another and terminate, due to the hindrance in their movement in space caused by the presence of the nanofiller as it was reported earlier.

Conclusions

In this investigation, synthesis and reaction kinetics of PMMA/organomodified MMT nanocomposites prepared by in situ bulk polymerization were studied. It was found that the presence of OMMT slightly enhance reaction rate and conversion versus time. The particular strongest effect of some type of OMMT was attributed to the bulk ammonium salt, used as the organic modifier and its influence on the effect of diffusion-controlled phenomena taking place during polymerization. Chemical reaction between the nanoparticles and the monomer/polymer does not seem to take place, while the T_g and the average molecular weight of the final materials were higher than that of pure PMMA.

Acknowledgements We would like to thank very much Southern Clay Products Inc. (Texas, USA) for a generous gift of the Cloisites used in this work, as well as Miss E. Panayotidou for carrying out the WAXD measurements.

References

1. Mai YW, Yu ZZ. Polymer nanocomposites. England: Woodhead Publishing Ltd; 2006.
2. Ahmadi SJ, Huang YD, Li W. Synthetic routes, properties and future applications of polymer-layered silicate nanocomposites. J Mater Sci. 2004;39:1919–25.
3. Okada A, Kawasumi M, Usuki A, Kojima Y, Kurauchi T, Kamigaito O. Nylon 6-clay hybrid. In: Schaefer DW, Mark JE. Polymer based molecular composites, vol 171. Materials Research Society Symposium Proceedings, Pittsburgh, 1990; p. 45–50.
4. Paul DR, Robeson LM. Polymer nanotechnology: nanocomposites. Polymer. 2008;49:3187–204.
5. Pavlidou S, Papaspyrides CD. A review on polymer-layered silica nanocomposites. Prog Polym Sci. 2008;33:1119–98.
6. Tjong SC. Structural and mechanical properties of polymer nanocomposites. Mater Sci Eng. 2006;R53:73–197.
7. Gao Z, Xie W, Hwu JM, Wells L, Pan WP. The characterization of organic modified montmorillonite and its filled PMMA nanocomposite. J Therm Anal Calorim. 2001;64:467–75.
8. Liaw JH, Hsueh TY, Tan TS, Wang Y, Chiao SM. Twin-screw compounding of poly(methyl methacrylate)/montmorillonite nanocomposites: effects of compounding temperature and matrix molecular weight. Polym Int. 2007;56:1045–52.
9. Zheng X, Jiang D, Wilkie CA. Methyl methacrylate oligomerically-modified clay and its poly(methyl methacrylate) nanocomposites. Thermochim Acta. 2005;435:202–10.
10. Tiwari RR, Natarajan U. Thermal and mechanical properties of melt processed intercalated poly(methyl methacrylate)-organoclay nanocomposites over a wide range of filler loadings. Polym Int. 2008;57:738–43.
11. Laachachi A, Ruch D, Addiego F, Ferriol M, Cochez M, Lopez Cuesta JM. Effect of ZnO and organo-modified montmorillonite on thermal degradation of PMMA nanocomposites. Polym Degrad Stab. 2009;94:670–8.
12. Si M, Goldman M, Rudomen G, Gelfer M, Sokolov JC, Rafailovich MH. Effect of clay type on structure and properties of PMMA/clay nanocomposites. Macromol Mater Eng. 2006; 291:602–11.
13. Kumar S, Jog JP, Natarajan U. Preparation and characterization of PMMA-clay nanocomposites via melt intercalation: the effect of organoclay on the structure and thermal properties. J Appl Polym Sci. 2003;89:1186–94.
14. Li Y, Zhao B, Xie S, Zhang S. Synthesis and properties of PMMA/MMT nanocomposites. Polym Int. 2003;52:892–8.
15. Xie T, Yang G, Fang X, Ou Y. Synthesis and characterization of poly(methyl methacrylate)/montmorillonite nanocomposites by in situ bulk polymerization. J Appl Polym Sci. 2003;89:2256–60.
16. Su S, Jiang DD, Wilkie CA. Methacrylate modofied clays and their polystyrene and poly(methyl methacrylate) nanocomposites. Polym Adv Technol. 2004;15:225–31.
17. Ingram S, Dennis H, Hunter I, Liggat J, McAdam C, Pethrick RA, Schaschke C, Thomson D. Influence of clay type on exfoliation, cure and physical properties of in situ polymerised poly(methyl methacrylate) nanocomposites. Polym Int. 2008;57:1118–27.
18. Qu X, Guan T, Liu G, She Q, Zhang L. Preparation, structural characterization and properties of PMMA/MMT nanocomposites by bulk polymerization. J Appl Polym Sci. 2005;97:348–57.
19. Dhibar AK, Mallick S, Rath T, Khatua BB. Effect of clay platelet dispersion as affected by the manufacturing technique on thermal and mechanical properties of PMMA-clay nanocomposites. J Appl Polym Sci. 2009;113:3012–8.
20. Demir MM, Memesa M, Castignolles P, Wegner G. PMMA/zinc oxide nanocomposites prepared by in situ bulk polymerization. Macromol Rapid Commun. 2006;27:763–70.
21. Zheng J, Zhu R, He Z, Cheng G, Wang H, Yao K. Synthesis and characterization of PMMA/SiO_2 nanocomposites by in situ suspension polymerization. J Appl Polym Sci. 2009;115:1975–81.
22. Xie XL, Li RKY, Liu QX, Mai YW. Structure-property relationship of in situ PMMA modified nano-sized antimony trioxide filled PVC nanocomposites. Polymer. 2004;45:2793–802.
23. Wu W, He T, Chen J, Zhang X, Chen Y. Study on in situ preparation of nano-calcium carbonate/PMMA composite particles. Mater Lett. 2006;60:2410–5.
24. Roman F, Montserrat S, Hutchinson JM. On the effect of montmorillonite in the curing reaction of epoxy nanocomposites. J Therm Anal Calorim. 2007;87:113–8.
25. Peila R, Malucelli G, Priola A. Preparation and characterization of UV-cured acrylic nanocomposites based on modified organophilic montmorillonites. J Therm Anal Calorim. 2009;97: 839–44.
26. Achilias DS, Bikiaris DN, Karavelidis V, Karayannidis GP. Effect of silica nanoparticles on solid state polymerization of poly(ethylene terephthalate). Eur Polym J. 2008;44:3096–107.
27. Zou DQ, Yoshida H. Size effect of silica nanoparticles on thermal decomposition of PMMA. J Therm Anal Calorim. 2010;99:21–6.
28. Leszczynska A, Pielichowski K. Application of thermal analysis methods for characterization of polymer/montmorillonite nanocomposites. J Therm Anal Calorim. 2008;93:677–87.
29. Achilias DS, Karabela MM, Sideridou ID. Thermal degradation and isoconversional kinetic analysis of light-cured dimethacrylate copolymers. J Therm Anal Calorim. 2010;99:917–23.
30. Achilias DS. Application of the differential scanning calorimetry in measuring of polymerization kinetics. Advantages and limitations. In: Lee JN, editor. Modern trends in macromolecular chemistry. New York: Nova Science Publishers, Inc; 2009.
31. Fan X, Xia C, Advincula RC. Grafting of polymers from clay nanoparticles via in situ free radical surface-initiated polymerization: monocationic versus bicationic initiators. Langmuir. 2003;19:4381–9.
32. Kim S, Wilkie CA. Transparent and flame retardant PMMA nanocomposites. Polym Adv Technol. 2008;19:496–506.
33. Achilias DS. A review of modeling of diffusion controlled polymerization reactions. Macromol Theory Simul. 2007;16: 319–47.
34. Verros GD, Latsos T, Achilias DS. Development of a unified framework for calculating molecular weight distribution in diffusion controlled free radical bulk homo-polymerization. Polymer. 2005;46:539–52.
35. Verros GD, Achilias DS. Modeling gel effect in branched polymer systems: free-radical solution homopolymerization of vinyl acetate. J Appl Polym Sci. 2009;111:2171–85.
36. Nikolaidis AK, Achilias DS, Karayannidis GP. Synthesis and characterization of PMMA/organomodified montmorillonite nanocomposites prepared by in situ bulk polymerization. Ind Eng Chem Res. in press. doi:10.1021/ie100186a.
37. Achilias DS, Verros GV. Modeling of diffusion-controlled reactions in free-radical solution and bulk polymerization: model validation by DSC experiments. J Appl Polym Sci. 2010;116: 1842–56.
38. Moad G, Solomon DH. The chemistry of radical polymerization. Second fully revised edition. The Netherlands: Elsevier; 2006.